AD-A039 976 CALIFORNIA UNIV BERKELEY DEPT OF CHEMICAL ENGINEERING F/G 7/3
VISCOELASTIC PROPERTIES OF ENTANGLED POLYMERS. III. THE TRANSIE--ETC(U)
MAY 77 S D HONG, D SOONG, M SHEN N00014-75-C-0955
UNCLASSIFIED TR-12 NL

| OF |
AD
A039976

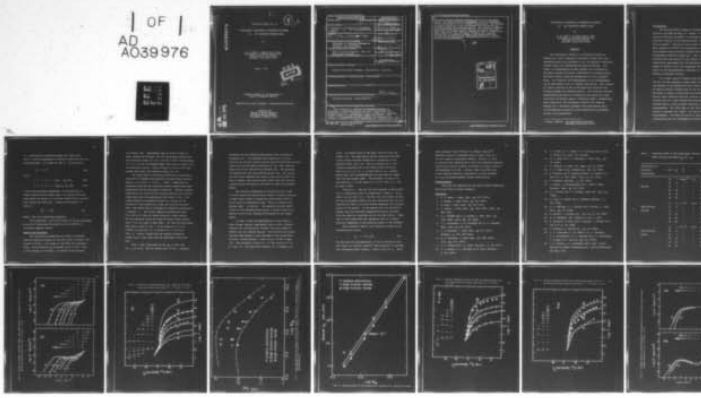

END

DATE
FILMED
6-77

Technical Report No. 12

VISCOELASTIC PROPERTIES OF ENTANGLED POLYMERS

III. THE TRANSIENT NETWORK MODEL

by

S. D. Hong, D. Soong and M. Shen
Department of Chemical Engineering
University of California
Berkeley, California 94720

May 1, 1977

Technical Report to be published in
Journal of Applied Physics

Prepared for
Office of Naval Research
800 North Quincy Street
Arlington, Virginia 22217

SECURITY CLASSIFICATION OF THIS PAGE (When Data Entered)

REPORT DOCUMENTATION PAGE

READ INSTRUCTIONS BEFORE COMPLETING FORM

1. REPORT NUMBER	2. GOVT ACCESSION NO.
3. RECIPIENT'S CATALOG NUMBER: (14) TR-12	
4. TITLE (and Subtitle): (6) Viscoelastic Properties of Entangled Polymers. III. The Transient Network Model.	5. TYPE OF REPORT & PERIOD COVERED: (9) Technical Report
	6. PERFORMING ORG. REPORT NUMBER: 12
7. AUTHOR(s): (10) S. D. Hong, D. Soong, M. Shen	8. CONTRACT OR GRANT NUMBER(s): (15) N00014-75-C-0955
9. PERFORMING ORGANIZATION NAME AND ADDRESS: Department of Chemical Engineering, University of California, Berkeley, California 94720	10. PROGRAM ELEMENT, PROJECT, TASK AREA & WORK UNIT NUMBERS: (11) 1 May 77
11. CONTROLLING OFFICE NAME AND ADDRESS: Office of Naval Research (Code 472), 800 N. Quincy Street, Arlington, Virginia 22217	12. REPORT DATE: May 1, 1977
	13. NUMBER OF PAGES: 30 (12) 32p.
14. MONITORING AGENCY NAME & ADDRESS (if different from Controlling Office)	15. SECURITY CLASS. (of this report): Unclassified
	15a. DECLASSIFICATION/DOWNGRADING SCHEDULE

16. DISTRIBUTION STATEMENT (of this Report)

Approved for public release: Distribution unlimited

AD 15644

17. DISTRIBUTION STATEMENT (of the abstract entered in Block 20, if different from Report)

18. SUPPLEMENTARY NOTES

404 601

19. KEY WORDS (Continue on reverse side if necessary and identify by block number)

Entangled Polymers, Viscoelasticity

20. ABSTRACT (Continue on reverse side if necessary and identify by block number)

The viscoelastic behavior of entangled polymers is modeled by a three dimensional transient network where the entangled points are considered to act as temporary crosslinks. Polymer chains are represented by beads and springs. The effect of entanglements on chain dynamic are introduced by assigning enhanced frictional coefficients to selected beads.

(over)

DD FORM 1 JAN 73 1473 EDITION OF 1 NOV 65 IS OBSOLETE
S/N 0102-014-6601 |

SECURITY CLASSIFICATION OF THIS PAGE (When Data Entered)

and extra elastic couplings between pairs of the entangled beads. The formation and disengagement of the entanglements can be envisioned to be in a dynamic equilibrium. The strength of elastic coupling is set to decrease with increasing the distance between the entangled points. The resulting modified Rouse-Bueche-Zimm matrix is solved for the relaxation times from which the dynamic moduli, relaxation moduli, steady-state shear compliance, and zero-shear viscosity are computed. Results are in excellent agreement with experimental data on monodisperse polystyrene, poly-(α)-methylstyrene, polyvinyl acetate and polybutadiene.

ALPHA

VISCOELASTIC PROPERTIES OF ENTANGLED POLYMERS.

III. THE TRANSIENT NETWORK MODEL

by

S. D. Hong *, D. Soong and M. Shen
Department of Chemical Engineering
University of California
Berkeley, California 94720

Abstract

The viscoelastic behavior of entangled polymers is modeled by a three dimensional transient network where the entangled points are considered to act as temporary crosslinks. Polymer chains are represented by beads and springs. The effect of entanglements on chain dynamic are introduced by assigning enhanced frictional coefficients to selected beads, and extra elastic couplings between pairs of the entangled beads. The formation and disengagement of the entanglements can be envisioned to be in a dynamic equilibrium. The strength of elastic coupling is set to decrease with increasing the distance between the entangled points. The resulting modified Rouse-Bueche-Zimm matrix is solved for the relaxation times from which the dynamic moduli, relaxation moduli, steady-state shear compliance, and zero-shear viscosity are computed. Results are in excellent agreement with experimental data on monodisperse polystyrene, poly-α-methylstyrene, polyvinyl acetate and polybutadiene.

---

* Present Address: Jet Propulsion Laboratory,
Pasadena, California 91103,

Introduction

The bead-and-spring theory of viscoelasticity for polymers expounded by Rouse (1), Bueche (2) and Zimm (3) has been eminently successful in elucidating the underlying molecular dynamics of an isolated polymer chain in a deformation gradient. Because of this success the model has been extended to predict the viscoelastic properties of bulk polymers whose molecular weights exceed their critical entanglement molecular weights (M_c). Most of the modified theories take into account of the effect of enhanced friction coefficients associated with the entangled beads (4-7). A number of authors (8,9) also recognized the elastic contribution of the entanglements in addition to the viscous effects of enhanced friction.

In a recent series of papers from this laboratory (10,11), we have proposed a simple model which incorporates the effects of the enhanced friction coefficients as well as specific elastic interactions of the entangled chains. Two types of elastic interactions are possible. One is the elastic force resulting from the coupling of the central molecule with all other neighboring molecules in the surrounding matrix, which we shall designate as the interchain entanglements. The other type is the central molecule looping around to entangle with itself, and may be called intrachain entanglements. The model was found to agree with the linear viscoelastic data for monodisperse polystyrene rather well.

Despite its apparent success in predicting experimental data, the model does require somewhat arbitrary division of the relative proportions of the inter- and intrachain entanglements. In this work, we shall examine the transient network model for entangled polymers in the bulk state. The entangled points are envisioned to act as temporary crosslinks,which are similar in nature to permanent chemical crosslinks except that their positions vary with time due to constant thermal motion. In the viscoelastic flow region, the entanglements undergo continuous formation and disengagement. The whole polymer network is therefore in dynamic equilibrium. Because of this transient entangled network, the rheological properties of high polymers exhibit a stronger molecular weight dependence of viscosity, a rubbery plateau region in the relaxation spectra, shear-rate-dependent viscosity phenomena, etc.

It should be pointed out that the idea of an entanglement network has previously been explored by a number of workers(12-17). The virtue of our model is its simplicity and its ability to predict experimental data to a high degree of accuracy. Ziabicki (16) has pointed out that in such networks elastic forces are transmitted through the entangled points, thus leading to long range correlation of the displacement. To obtain an exact solution of this problem would require the knowledge of the distribution function of all of the molecules in the network. In our case, we have resorted to an approximate solution of the problem by

using the original framework of the RBZ theory, which is really valid for a single chain problem. Since the multi-chain problem, though rigorously posed, is all but mathematically intractable at this time, we feel justified to use the simpler (if more approximate) approach in an effort to elucidate the salient features of the molecular dynamics of entangled bulk polymers.

Theory

The entanglement network proposed is depicted in Fig. 1, where all the molecules are coupled together to form a transient network. The formation of entanglements is a random process, thus spacings between adjacent entangled points along a chain are not the same and they change with time as a result of thermal motions. However, for simplicity, it is reasonable to assume that all the entangled points are on the average equally spaced.

The effects of entanglement on the motion of a polymer molecule are twofold. First, for a given molecule (e.g., the center heavy-lined molecule in Fig. 1) to move in the network all the surrounding chains entangled to it have to be dragged along. This has the effect of increasing the frictional coefficients of the entangled points, i.e., enhanced friction. Second, the entangled surrounding molecules can exert elastic forces on the central molecule at the entangled points. Since all the entangled points on the central molecule are coupled through the network, the

elastic force on a given entangled point is transmitted through the network and can affect the motion of the other entangled points. The coupling force is expected to diminish as the distance between the entangled points increase because the force must on the average be transmitted through a larger number of chains in the network. Using the bead-and-spring representation, the proposed entangled polymer chain is shown in Fig. 2.

Following the formulation of RBZ theory, the equation of motion of an untangled bead B is,

$$\dot{X}_k = V^s_{xk} - \frac{KT}{f_B}\frac{\partial \ln\psi}{\partial X_k} - \frac{3KT}{f_B\langle b_o^2\rangle}(-X_{k+1} + 2X_k - X_{k-1}) \qquad (1)$$

where $k \neq 0, N$, N is the total number of beads of the chain and $\langle b_o^2\rangle$ is the mean square end-to-end distance of a statistical segment. X_k and $\dot{X}_k$ are respectively the x-component of the coordinates and velocity of the kth bead. V^s_{xk} is the velocity of medium surrounding the kth bead, f_B is the frictional coefficient of the unentangled bead, ψ is the distribution function of the chain segment.

For an entangled bead i, the frictional coefficient, f_{Ai}, has a higher value than f_B because of the retardation effect of the entanglement. The chain segments between any two entanglements are constituents of the whole network. They and the surrounding molecules in effect from a closed loop, as shown in Fig. 2b. Displacing bead i and j from

their equilibrium positions will result in an elastic force to counteract this displacement. This elastic force may be given as

$$\sum_{j=1}^{N_e} \frac{3KT\alpha}{< b_{ij}^2 >} (X_j - x_j^I) \qquad (2)$$

where N_e is the total number of entangled points on the given molecule and

$$<b_{ij}^2> = |i-j|<b_o^2> \qquad (3)$$

is the mean square end-to-end distance between i and j. α is a parameter to account for the fact that the entanglement is not as effective as a permanent crosslink in transmitting force due to the fact that entangled chains can slip by each other. The value of α is therefore between 0 and 1, and is expected to be different for different entanglement points. However, as a first approximation it is assumed to be a constant for our calculations.

The equation of motion for an entangled bead A at X_j now becomes

$$\dot{X}_j = V_{xj}^s - \frac{KT}{f_{Aj}} \frac{\partial \ln \psi}{\partial x_j} - \frac{3KT}{f_{Aj}<b_o^2>} (-X_{j+1} + 2X_j - X_{j-1})$$

$$- \frac{3KT}{f_{Aj}<b_o^2>} \sum_{i=1}^{N_e} \epsilon_{ij} (X_j - X_i^I) \qquad (4)$$

where

$$\varepsilon_{ji} = \frac{\alpha}{|j-i|} \tag{5}$$

and $j \neq i \neq k$, f_{Aj} is the frictional coefficient of entangled bead at X_j. Expressed in matrix notation, the equations of motion for a single chain can be wirtten as

$$\dot{\underset{\sim}{X}} = \underset{\sim}{V}^s_x - \mathcal{D}_B \, \underset{\sim}{D}^{-1} \, \frac{\partial \ln \psi}{\partial \underset{\sim}{X}} - \sigma_B \, \underset{\sim}{D}^{-1} \, \underset{\sim}{Z}_e \, \underset{\sim}{X} \tag{6}$$

where $\dot{\underset{\sim}{X}}$ and $\underset{\sim}{X}$ are column vectors of velocity and position of the beads, resepctively; $\underset{\sim}{V}^s_x$ is the x-component of the velocity of the surrounding medium, $\mathcal{D}_B = \frac{KT}{f_B}$ is the diffusion coefficient, $\sigma_B = \frac{3KT}{\langle b_o^2 \, f_B \rangle}$, and $\underset{\sim}{D}^{-1}$ is the inverse of the matrix $\underset{\sim}{D}$:

$$\underset{\sim}{D} = \begin{bmatrix} 1 & & & & & & \\ \delta_2^1 & 1 & & & & & \\ & \delta_4^2 & 1 & & & & \\ & & \ddots & \ddots & & & \\ & & & \delta_j^I & 1 & \ddots & \\ & & & & \ddots & \ddots & 1 \end{bmatrix} \tag{7}$$

where $\delta_j^I = \frac{f_{Aj}^I}{f_B}$. $\underset{\sim}{Z}_e$ is the modified version of the nearest neighbor matrix for an entangled polymer chain (3), and for a chain with alternating entangled and unentangled intervening beads,

$$\underset{\sim}{Z}_e = \begin{bmatrix} 1 & -1 & 0 & 0 & 0 & 0 & -- \\ -1 & 2+\gamma_2 & -1 & -\varepsilon_{24} & 0 & -\varepsilon_{26} & -- \\ 0 & -1 & 2 & -1 & 0 & 0 & -- \\ 0 & -\varepsilon_{42} & -1 & 2+\gamma_4 & -1 & -\varepsilon_{46} & -- \\ 0 & 0 & 0 & -1 & 2 & 1 & -- \\ - & - & - & - & - & - & - \\ - & - & - & - & - & - & - \end{bmatrix} \tag{8}$$

where

$$\gamma_j = \sum_{\substack{i=1 \\ j \neq (i-1),i,(i+1)}}^{N+1} \varepsilon_{ij} \tag{9}$$

The equation of motion, Eq. 6, is very similar to the one derived by Zimm (3) except that the matrix $\underset{\sim}{H}$, which accounts for the hydrodynamic interaction of the solvent, is replaced by the matrix $\underset{\sim}{D}^{-1}$ and $\underset{\sim}{Z}_e$. Following Zimm, the relaxation times age given by

$$\tau_p = \frac{1}{2\sigma_B \lambda_p} \tag{10}$$

where λ_p is the p-th eigenvalue of $\underset{\sim}{D}^{-1}\ \underset{\sim}{Z}_e$.

The eigenvalues (λ_p's) and consequently the relaxation times (λ_p's) are dependent on the choice of the total number of beads (N+1) to represent a molecule. It has been shown previously (10,11) that this arbitrariness can be removed

if the reduced frictional coefficient

$$\delta_j^I = \frac{N_e}{N+1} \delta_j^I \tag{11}$$

and the reduced relaxation times

$$\tau'_p = \frac{N_e^2}{(N+1)N} \frac{1}{\lambda_p} \tag{12}$$

are used for subsequent calculations of the viscoelastic properties.

We have thus developed the equation of motion for a polymer chain in the entanglement network. Instead of considering the detailed kinematics of the chain (16), we made an assumption that the effects of entanglements can be treated by additional frictional and elastic interaction. The normal coordinate approach is still applicable to solving the modified RBZ matrix. We have also assumed that the positions of the entangled beads are fixed and are equally spaced for the ease of computation. Realistically, however, the entangled beads are probably randomly distributed along the chain, but the need to introduce such subleties is dubious. As for the mathematical expression of the frictional coefficients, we adopted the scheme used in previous publications[7,10,11]. The molecular weight dependence is introduced to the reduced frictional coefficient in three ways. (1) high-friction coefficient entangled beads near the chain middle,

(2) high-friction coefficient beads near chain ends and (3) uniform enhancement of friction coefficient for all entangled beads. For cases (2) and (3) $\delta_j^{I'}$ is given as

$$\delta_j^{I'} = a\, I^b \tag{13a}$$

where

$$I = 1, 2, 3 \ldots N_e/2 \quad (N_e \text{ even}) \tag{13b}$$

$$I = 1, 2, 3 \ldots (N_e+1)/2 \quad (N_e \text{ odd}) \tag{13c}$$

a and b are adjustable parameters, the distribution is called "high-friction inside" when I is counted from both ends toward the center, it is called "high-friction outside" when counted the other way. "Uniform distribution" is given by

$$\delta_j^{I'} = c\, N_e^d \tag{14}$$

where c and d are adjustable parameters.

The eigenvalues λ_p's of the matrix $\underset{\sim}{D}^{-1}\, \underset{\sim}{Z}_e$ can be solved by a set of subroutines available at the University of California computer center.

Results and Discussion

The viscoelastic properties are readily calculated from the relaxation spectra by the well known relations (10). Values of $\delta_j^{I'}$ and α are chosen to calculate the relaxation times. For polystyrene M_e is assumed to be 1.7×10^4. This is the average of the range $1.5\text{-}1.8 \times 10^4$ cited by Porter

and Johnson (18). Experimental data on dynamic moduli by Onogi, Masuda and Kitagawa (19) for monodisperse polystyrene with molecular weight of 1.67, 2.67 and 5.8×10^5 (corresponding to 7, 10, 16 and 34 entangled beads) were used to compare with the predicted results. Stress relaxation data for the same polymer were taken from Akovali's paper (20, 21).

All three cases of frictional coefficient distribution give good fit between the predicted and experimental storage moduli, $G'(\omega)$ (Figs. 3, 4 and 5). Table 1 summarizes the parameters used and the calculated reduced steady-state shear compliances and the zero-shear viscosities. However, uniform distribution and high-friction outside cases do not give good comparisons with the experimental loss moduli, $G''(\omega)$. The former predicts an excessive minimum as a result of the relaxation times clustering at both the long and the short ends. This defect may in principle be removed by introducing a variable α. The latter compares favorably with both $G'(\omega)$ and $G''(\omega)$ data for higher molecular weight samples, but the predicted curves for lower molecular weight samples tend to lie too close to each other. The high-friction-inside case gives a good fit for α in the range of 0.1 to 0.5. However, an excellent fit is obtained for $0.16<\alpha<0.21$ (Fig. 5). Figure 6 shows that the computed relaxation curves, $E_r(t)$, also agree with the experimental data very well.

Figs. 7 and 8 show plots of log J_{eR} vs log M and log η_o vs log M. The two dashed lines in Fig. 7 represent

boundaries of the scattered experimental data collected by Graessley (22). The agreement with experiment is fairly good for the uniform friction and the high-friction-outside cases except for the discrepancy mentioned for the lower molecular weight end of the high-friction-outside case. The agreement is excellent for the high-friction-inside case. The results from this work together with those of the previous work (10) seem to suggest that high-friction inside case with variable coupling spring constants is the best one among the proposed models.

The arbitrary assumptions of uniform friction, high-friction outside and high-friction inside is aimed at finding a simple model capable of predicting experimental results while retaining computationl case. They are actually only extreme cases. In reality, the enhanced friction coefficients of the entangled points may be a varying function of position which is not regularly distributed as the chosen models.

In order to test the applicability of this model to other polymer systems, experimental data of poly (α-methylstyrene) (23) and poly(vinyl acetate) (24) were chosen to compare with the computed results. The high-friction-insdie case was used because it gave the best fit for polystyrene. For poly (α-methylstyrene) a value of M_e = 10,000 is used (23). The agreement is good for α in the range of 0.3 to 0.5 (Fig. 9). For poly(vinyl acetate), M_e is assumed to be

9,400, an average value of the data cited by Porter and Johnson (4). The experimental stress relaxation data show a more gradual terminal transition in comparison to our computed curves (Fig. 10). This is probably due to the residual polydispersity in the rough polymer fractions used (H.I.=1.1 to 1.2). α in this case is 0.1. Dynamic moduli data (25) on polybutadiene are also used for comparison with the present model. The agreement is seen to be very good for α in the range of 0.1 to 0.2 (Fig. 11). The M_e used is 3000.

Values of α used for all four polymers to obtain best fits to experimental data are summarized in Table 2. In all cases, we find that $0<\alpha<1$. The fact that the elastic springs for the entanglement network all have strengths that are only fractions of these of the main chains emphasizes the transient nature of the network. If the network were all convalently bonded, then one would have expected the spring constants to be the same for crosslinks and for the main chains. Lodge (14) in fact showed that the relaxation time of a network would be independent of the molecular weight of the polymers.

Also included in Table 2 are literature values of the characteristics ratios

$$C_\infty = \langle r^2 \rangle / nl^2 \qquad (15)$$

for the same four macromolecules. It is of interest to note that there is a similar trend for both parameters to increase with increasing chain rigidity. Higher values of C_∞ would

imply enhanced "front factors" in rubbery networks[26], therefore should be consistent with a higher value of α for our transient entangled networks. However, in view of the fact that characteristic ratios are generally obtained from dilute solution studies, one would not expect a strict correspondence with the α factors taken from bulk data. A more detailed molecular significance of this parameter is to be elucidated pending further investigation.

Acknowledgement

This work was supported by the Union Carbide Corporation, and by the Office of Naval Research.

References

1. P. E. Rouse, J. Chem. Phys., 21, 1272 (1953).
2. F. Bueche, J. Chem. Phys., 22, 603 (1954).
3. B. Zimm, J. Chem. Phys., 24, 269 (1956).
4. F. Bueche, J. Chem. Phys., 20, 1959 (1952); ibid., 25, 599 (1956).
5. A. J. Chompff and J. A. Duiser, J. Chem. Phys., 45, 1505 (1966); ibid., 48, 235 (1968).
6. G. V. Vinogradov, V. H. Prkrovsky and Yu. G. Yanovsky, Rheol. Acta, 11, 258 (1972).
7. P. G. DeGennes, J. Chem. Phys., 55, 572 (1971); Macromol., 9, 587, 594 (1976).
8. W. W. Graessley, J. Chem. Phys., 47, 1942 (1967); ibid., 54, 5143 (1971).
9. W. C. Forsman and H. S. Grand, Macromol., 5, 289 (1972).
10. D. R. Hansen, M. C. Williams and M. Shen, Macromol., 9, 354 (1976).

11. S. D. Hong, D. R. Hansen, M. C. Williams and M. Shen J. Polymer Sci.-Phys. Ed. in press.

12. M. S. Green and A. V. Tobolsky, J. Chem. Phys., 14, 80 (1946).

13. M. Yamamoto, J. Phys. Sco. Japan, 11, 413 (1956).

14. A. S. Lodge, Trans. Faraday Soc., 52, 120 (1956).

15. A. Ziabicki and R. Takserman-Krozer, J. Polymer Sci., Part A-2, 7, 2005 (1969); ibid., 8, 321 (1970).

16. A. Ziabicki, Macromol., 7, 501 (1974).

17. J. Schurz, A. Mavrommatakos and K. Muller, Angew. Macromol. Chem., 36, 181 (1974).

18. R. S. Porter and J. F. Johnson, Chem. Rev., 66, 1511 (1966).

19. S. Onogi, T. Masuda and K. Kitagawa, Macromol., 3, 109 (1970).

20. A. V. Tobolsky, J. J. Aklonis and G. Akovali, J. Chem. Phys., 42, 723 (1965).

21. G. Akovali, J. Polymer Sci., Part A-2, 5, 875 (1967).

22. W. W. Graessley, Adv. Polymer Sci.,16, 1 (1974).

23. T. Fujimoto, N. Ozaki and M. Nagasawa, J. Polymer Sci., Part A-2, 6, 129 (1968).

24. K. Ninomiya, J. Colloid Sci., 14, 49 (1959).

25. G. V. Vinogradow, A. Ya. Malkin, Yu. G. Yanovskii, E. K. Borinsenkova, B. V. Yarlykov and G. V. Berezhnaya, J. Polymer Sci., Part A-2, 10, 1061 (1972).

26. J. J. Aklonis, W. J. MacKnight and M. Shen, "Introduction to Polymer Viscoelasticity", Wiley-Interscience, New York, 1972.

Table 1. Parameters Used in the Entanglement Network Model and the Calculated J_{eR} and η_o.

Distribution of Frictional Coefficients	(N+1)	N_e	$\delta_j^{I'}$		J_{eR}	η_o
	19	3	$0.06N_e^{3.5}$	0.16	.434	1.25
	19	4	"	"	.421	3.48
Uniform	31	7	"	"	.298	2.95x10
	32	10	"	"	.220	$1.12x10^2$
	33	16	"	"	.140	$5.97x10^2$
	69	34	"	"	.063	$7.59x10^3$
	19	3	$1.0\ I^4$	0.16	.803	4.06
High Friction	19	4	"	"	.766	4.25
Outside	31	7	"	"	.545	2.72x10
	32	10	"	"	.537	$1.30x10^2$
	33	16	"	"	.376	$7.39x10^2$
	69	34	"	"	.186	$1.18x10^4$
	19	3	$1.0\ I^4$	0.16	.331	.971
High Friction	19	4	"	"	.465	2.27
Inside	31	7	"	"	.333	1.56x10
	32	10	"	"	.268	6.10x10
	33	16	"	"	.186	$3.98x10^2$
	69	34	"	"	.101	$7.67x10^3$

Table 2. The α Factors and the Characteristic Ratios of Polymer Chains

Polymer	α	C_∞
Poly(α-methyl Styrene)	0.3 - 0.5	13.0 [a]
Polystyrene	0.16 - 0.21	9.9 - 10.2 [b]
Poly(vinyl Acetate)	0.1	8.9 - 9.2 [b]
Polybutadiene	0.1	4.7 - 5.1 [c,d]

a. T. Fujimoto, N. Ozaki and M. Nagasawa, J. Polymer Sci., Part A-2, 6, 129 (1968).

b. P. J. Flory, "Statistical Mechanics of Chain Molecules", Interscience, New York, 1969.

c. G. Moraglio, Eur. Polymer J., 1, 103 (1965).

d. M. Abe and H. Fujita, J. Phys. Chem., 69, 3263 (1965).

Captions of the figures

Fig. 1. Polymer chains forming an entanglement network. The heavy-lined chain represents the central chain.

Fig. 2 Schematic representation of the entanglement network. (a) The central chain is represented by beads connected by springs in solid lines. The broken lines represent the coupling springs. (b) The segment between entangled beads i, and j is connected to the surrounding molecules to form a closed loop.

Fig. 3 Plots of dynamic storage moduli $G'(\omega)$ and loss moduli $G''(\omega)$ vs. frequency for the uniform friction case. $\delta_j^{I'} = 0.06N_e^{3.5}$ and $\alpha = 0.16$. The discrete lines at the top of the figures represent the calculated relaxation times. Numerals at the bottom of each curve represent numbers of entanglements of samples.

Fig. 4 Plots of dynamic storage moduli and loss moduli vs frequency for the high-friction-outside case with $\delta_j^{I'} = I^4$ and $\alpha = 0.16$.

Fig. 5 Plots of dynamic storage moduli and loss moduli vs frequency for the high-friction-inside case with $\delta_j^{I'} = I^4$ and $\alpha = 0.16$.

Fig. 6 Plots of relaxation moduli vs time for the high-friction-inside case with $\delta_j^{I'} = I^4$ and $\alpha = 0.16$.

Fig. 7 Log-log plot of the reduced steady-state shear compliance vs molecular weight. The dashed lines represent the range of scatter of literature data for monodisperse polystyrenes (1).

Fig. 8 Log-log plots of zero-shear-rate viscosity vs molecular weight.

Fig. 9 Stress relaxation data for poly-α-methylstyrene (23) for the high-friction-inside case with $\delta_j^{I'} = I^4$ and $\alpha = 0.4$.

Fig. 10 Stress relaxation data for polyvinyl acetate (24) for the high-friction-inside case with $\delta_j^{I'} = I^4$ and $\alpha = 0.1$.

Fig. 11 Dynamic moduli for monodisperse polybutadine (25) for the high-friction-inside case with $\delta_j^{I'} = I^4$ and $\alpha = 0.2$.

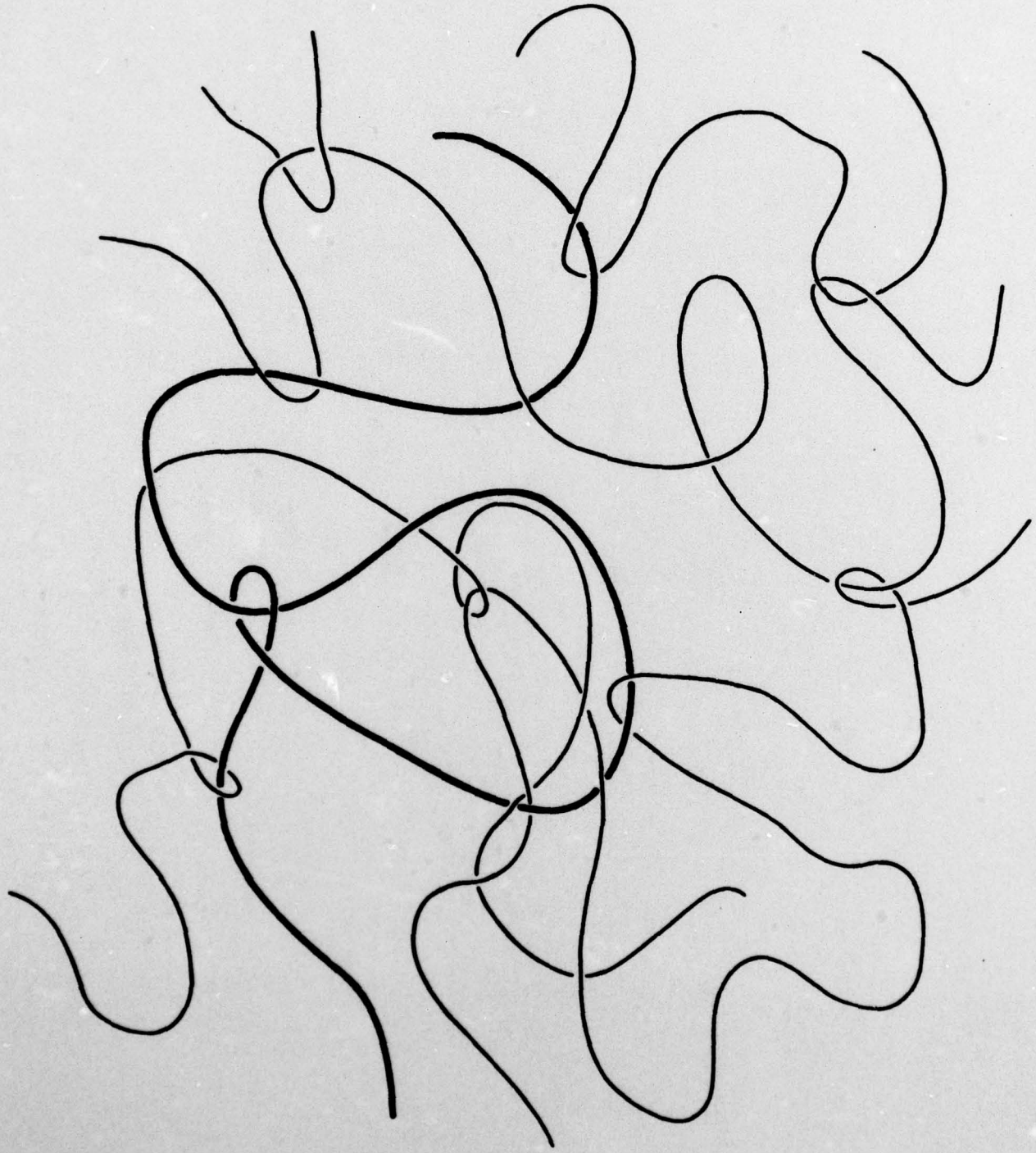

Fig. 1. Polymer chains forming an entanglement network. The heavy-lined chain represents the central chain.

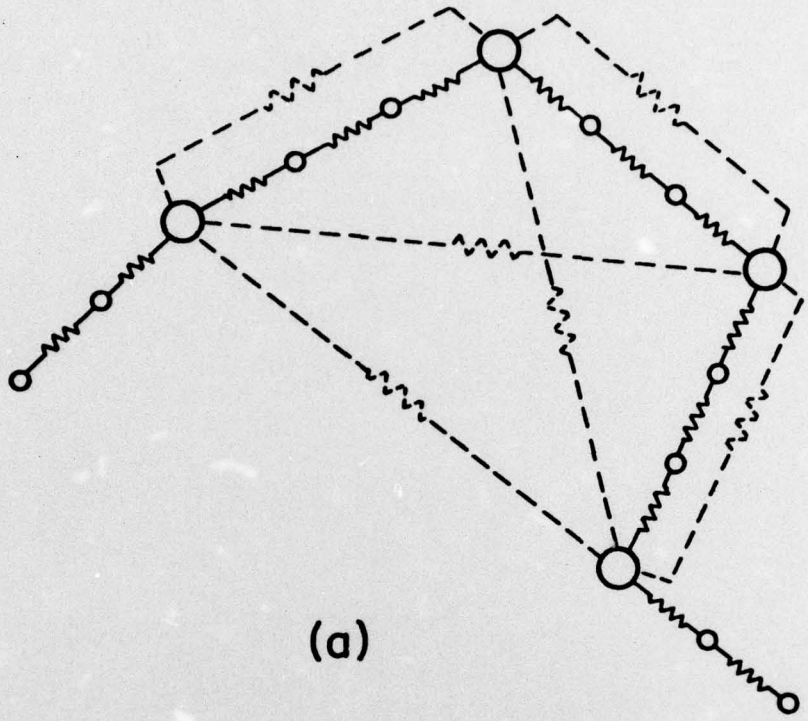

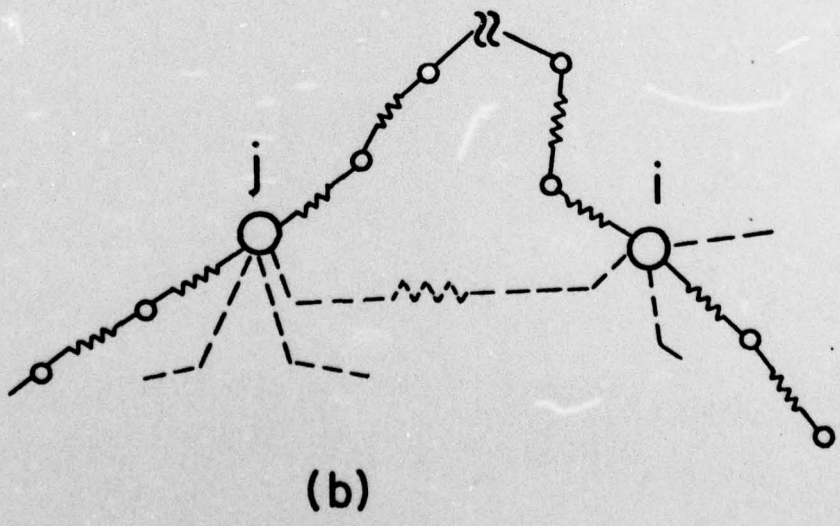

Fig. 2. Schematic representation of the entanglement network. (a) The central chain is represented by beads connected by springs in solid lines. The broken lines represent the coupling springs. (b) The segment between entangled beads i, and j is connected to the surrounding molecules to form a closed loop.

Fig. 3 Plots of dynamic storage moduli G'(ω) and loss moduli G"(ω) vs. frequency for the uniform friction case. $\delta_j^{I'} = 0.06N_e^{3.5}$ and $\alpha = 0.16$. The discrete lines at the top of the figures represent the calculated relaxation times. Numerals at the bottom of each curve represent numbers of entanglements of samples.

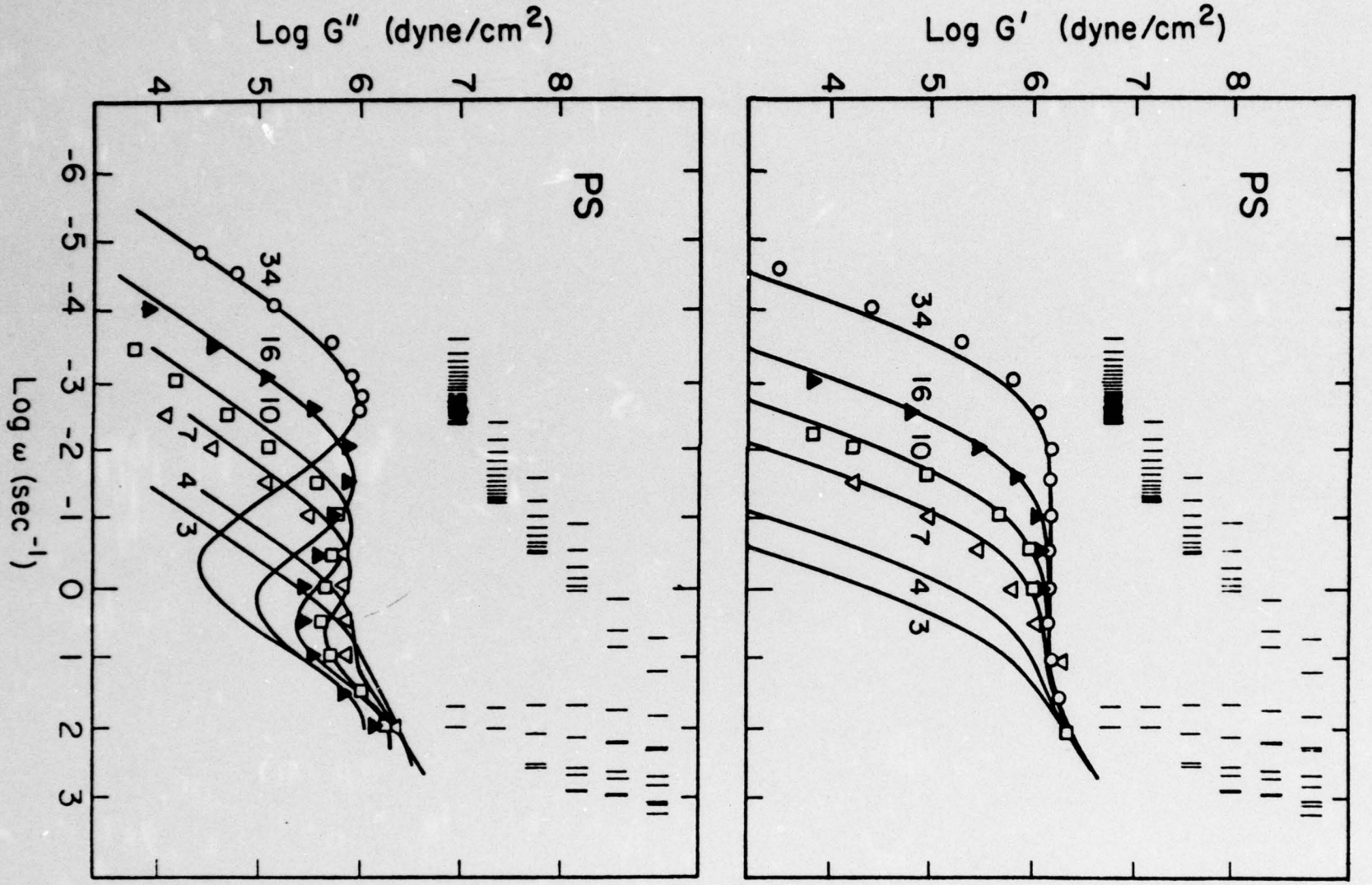

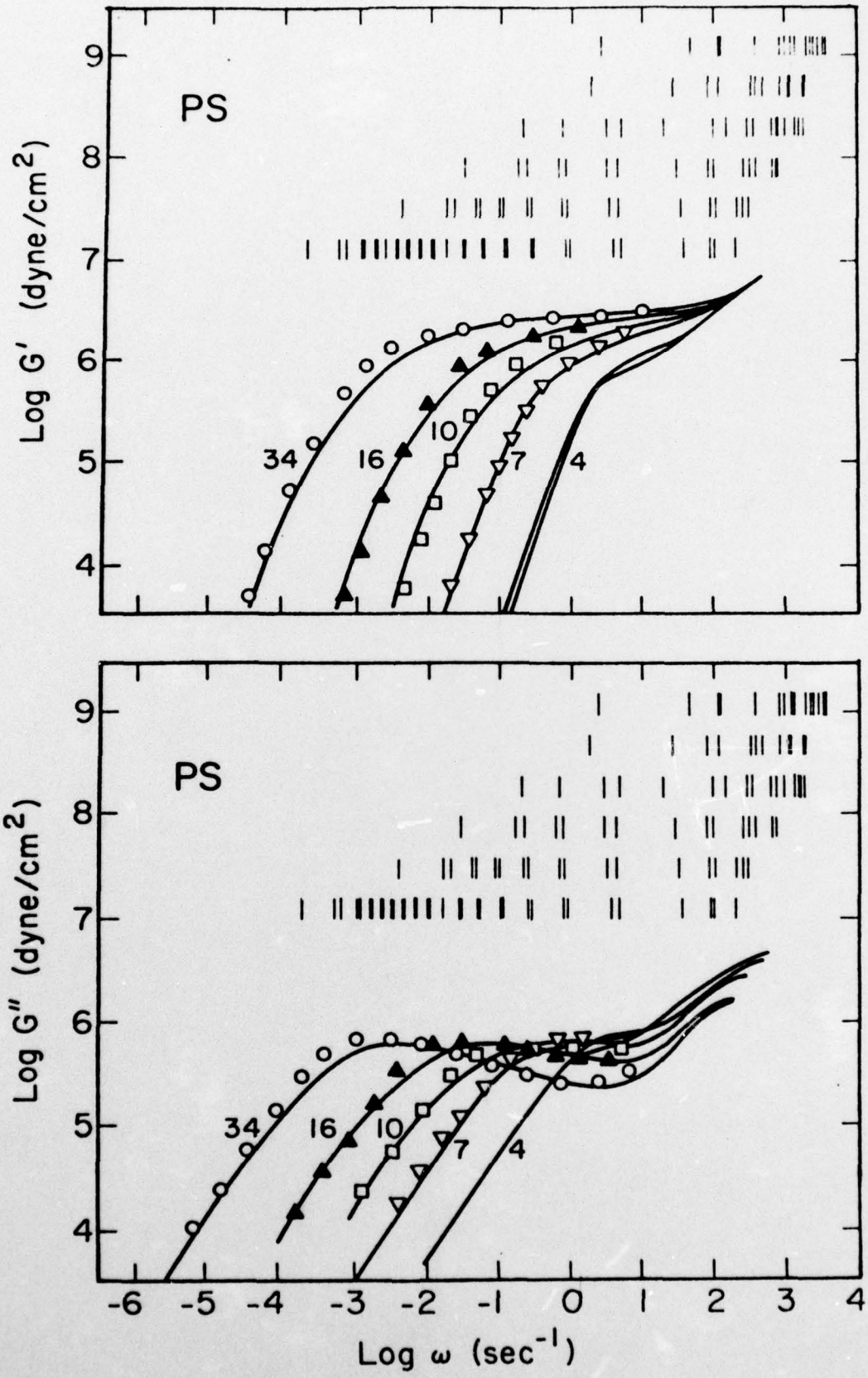

Fig. 4 Plots of dynamic storage moduli and loss moduli vs. frequency for the high-frequency for the high-friction-outside case with $\delta_j^{I'} = I^4$ and $\alpha = 0.16$.

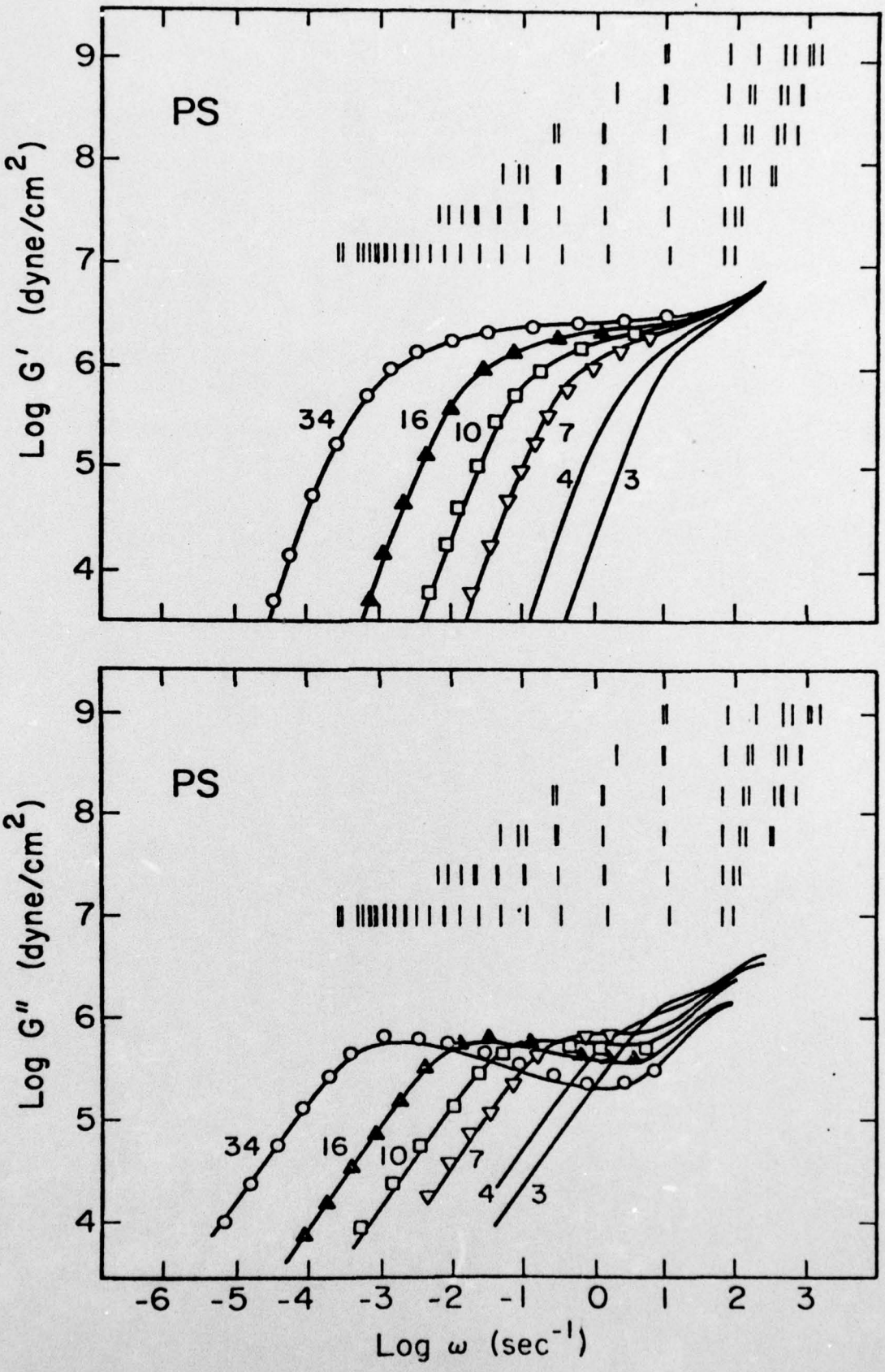

Fig. 5 Plots of dynamic storage moduli and loss moduli vs. frequency for the high-friction-inside case with $\delta_j^{I'} = I^4$ and $\alpha = 0.16$.

Fig. 6 Plots of relaxation moduli vs. time for the high-friction-inside case with $\delta_j^{I'} = I^4$ and $\alpha = 0.16$.

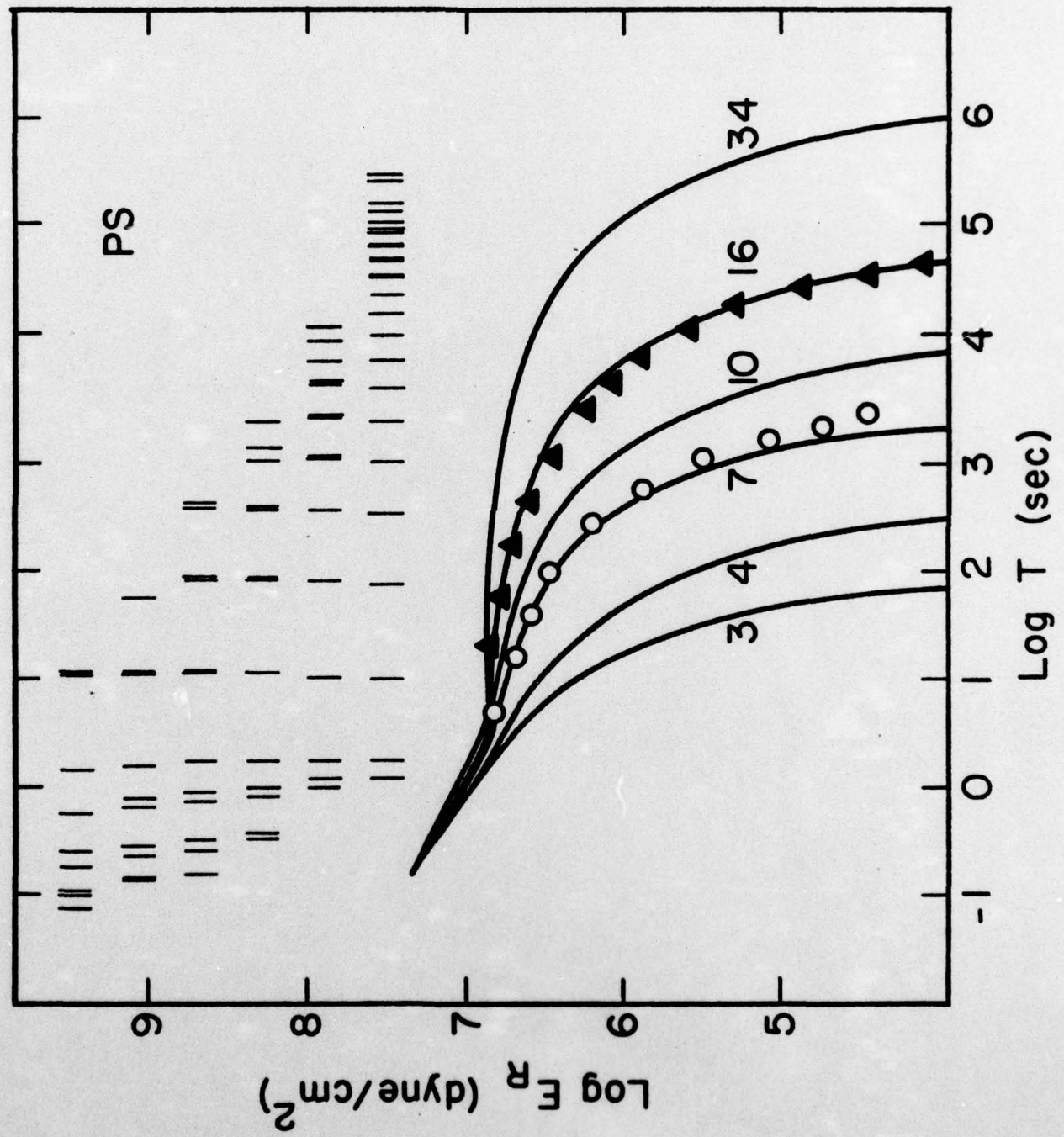

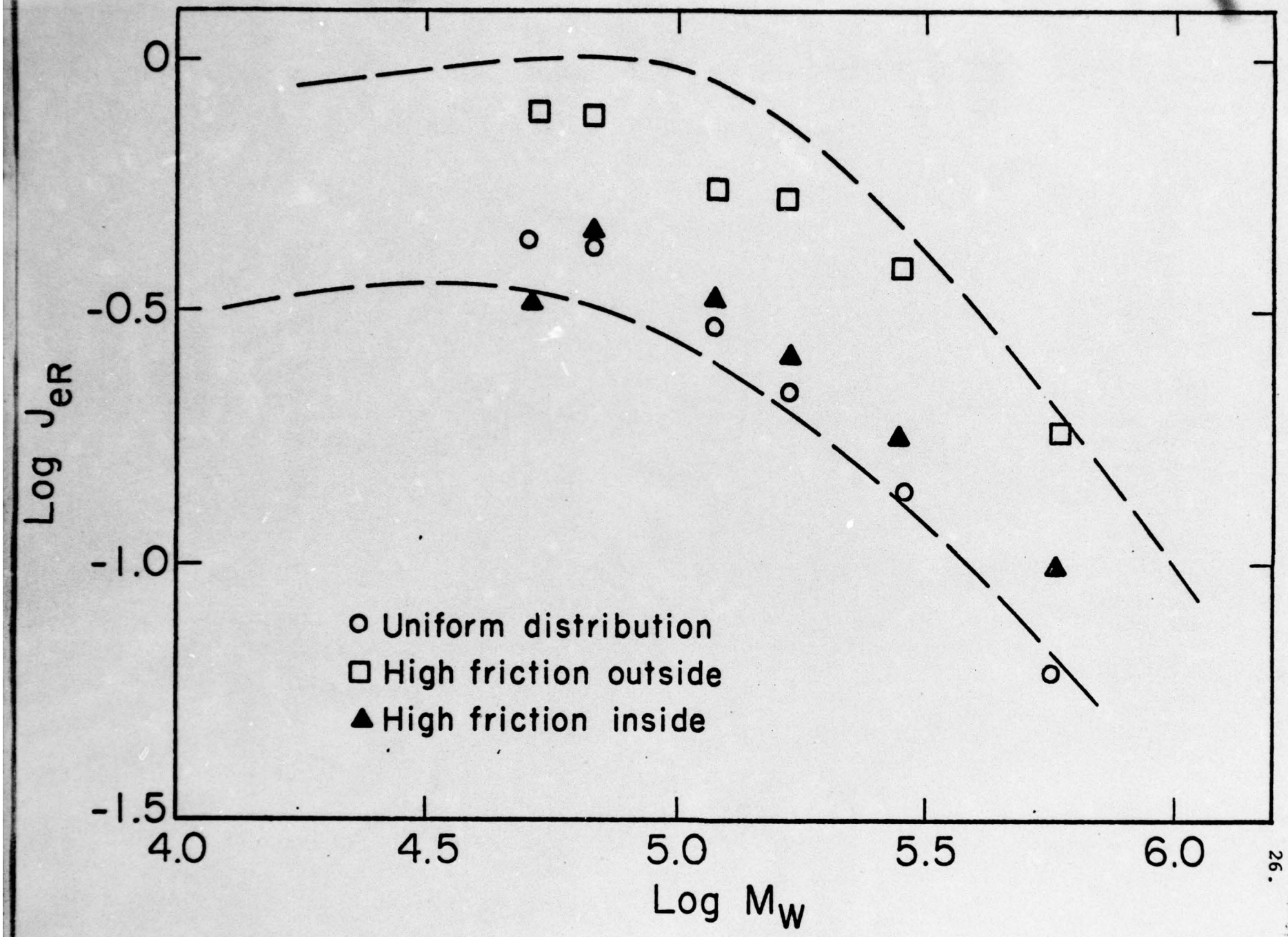

Fig. 7 Log-log plot of the reduced steady-state shear compliance vs. molecular weight. The dashed lines represent the range of scatter of literature data for monodisperse polystyrenes(1).

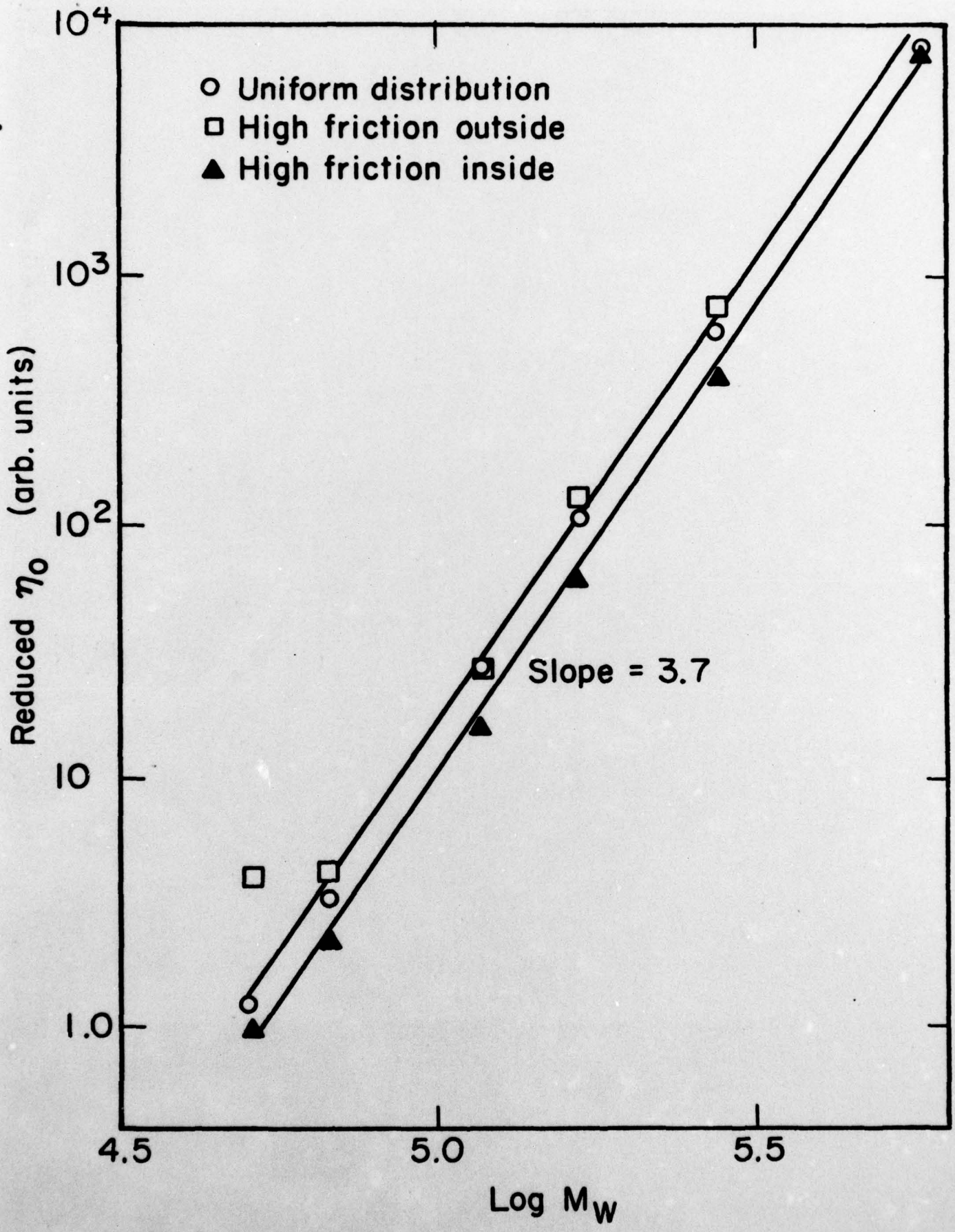

Fig. 8 Log-log plots of zero-shear-rate viscosity vs. molecular weight.

Fig. 9 Stress relaxation data for poly-α-methylstyrene for the high-friction-inside case with $\delta_j^{I'} = I^4$ and $\alpha = 0.4$.

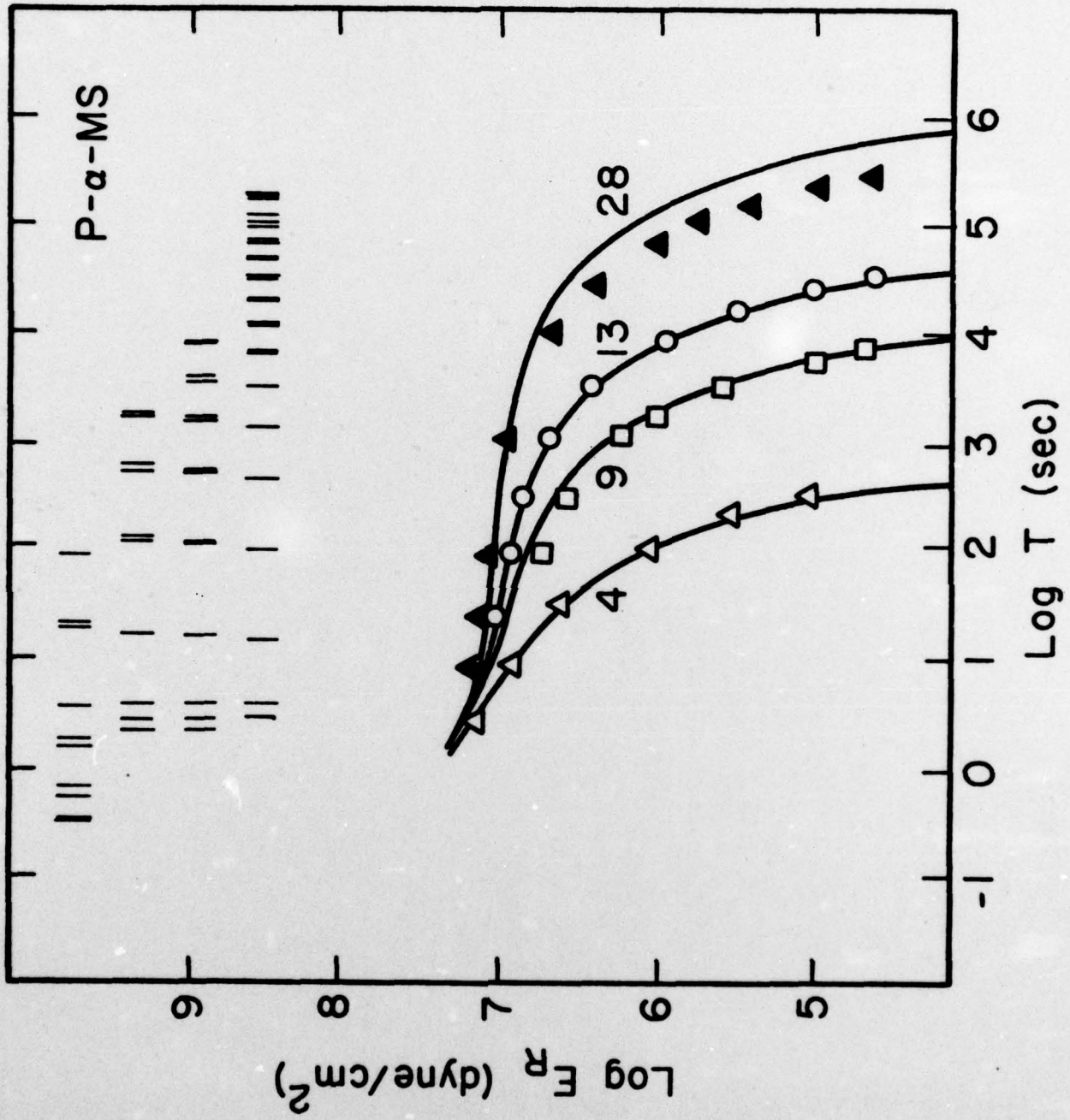

Fig. 10 Stress relaxation data for polyvinyl acetate (24) for the high-friction-inside case with $\delta_j^{I'} = I^4$ and $\alpha = 0.1$.

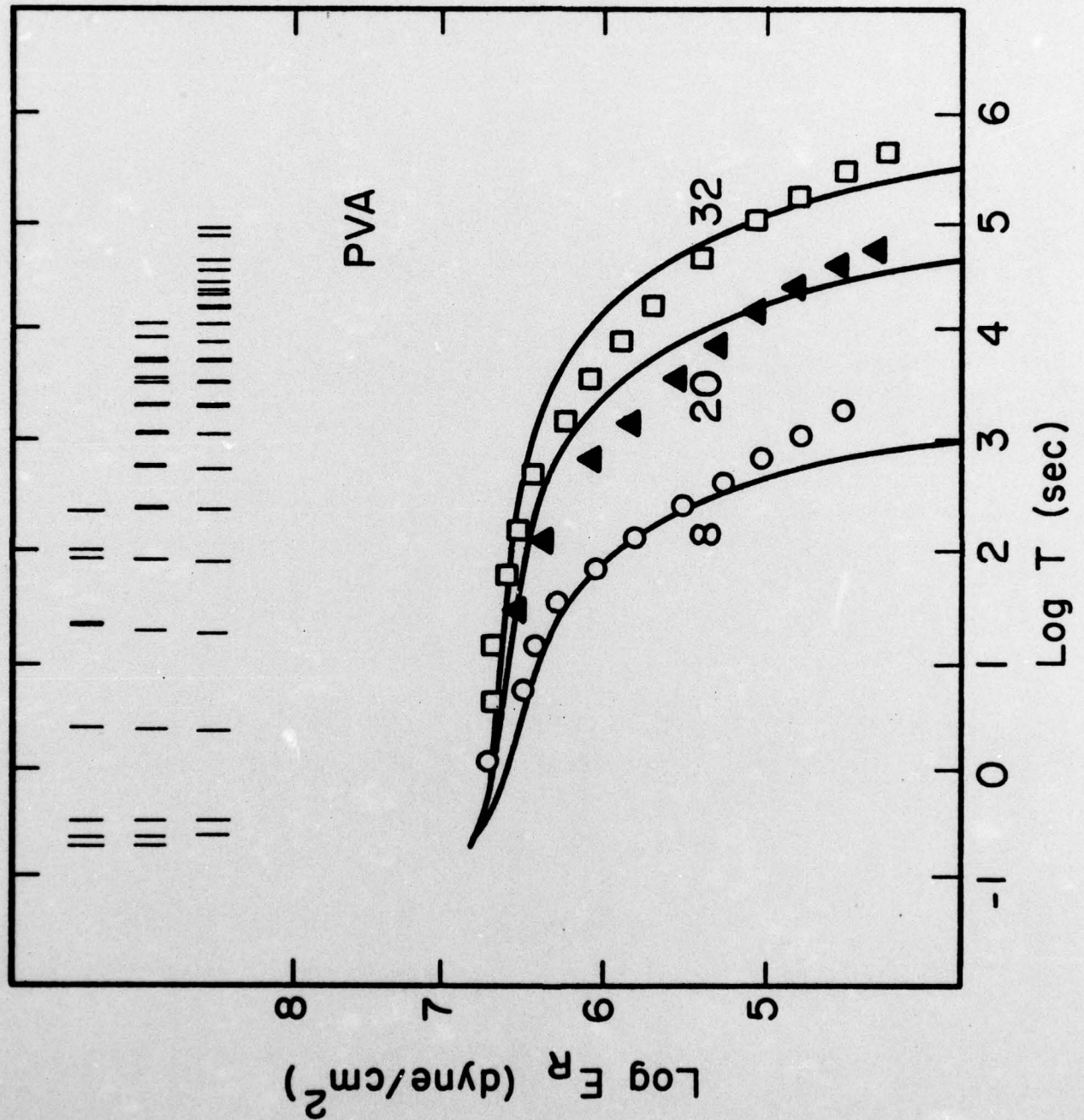

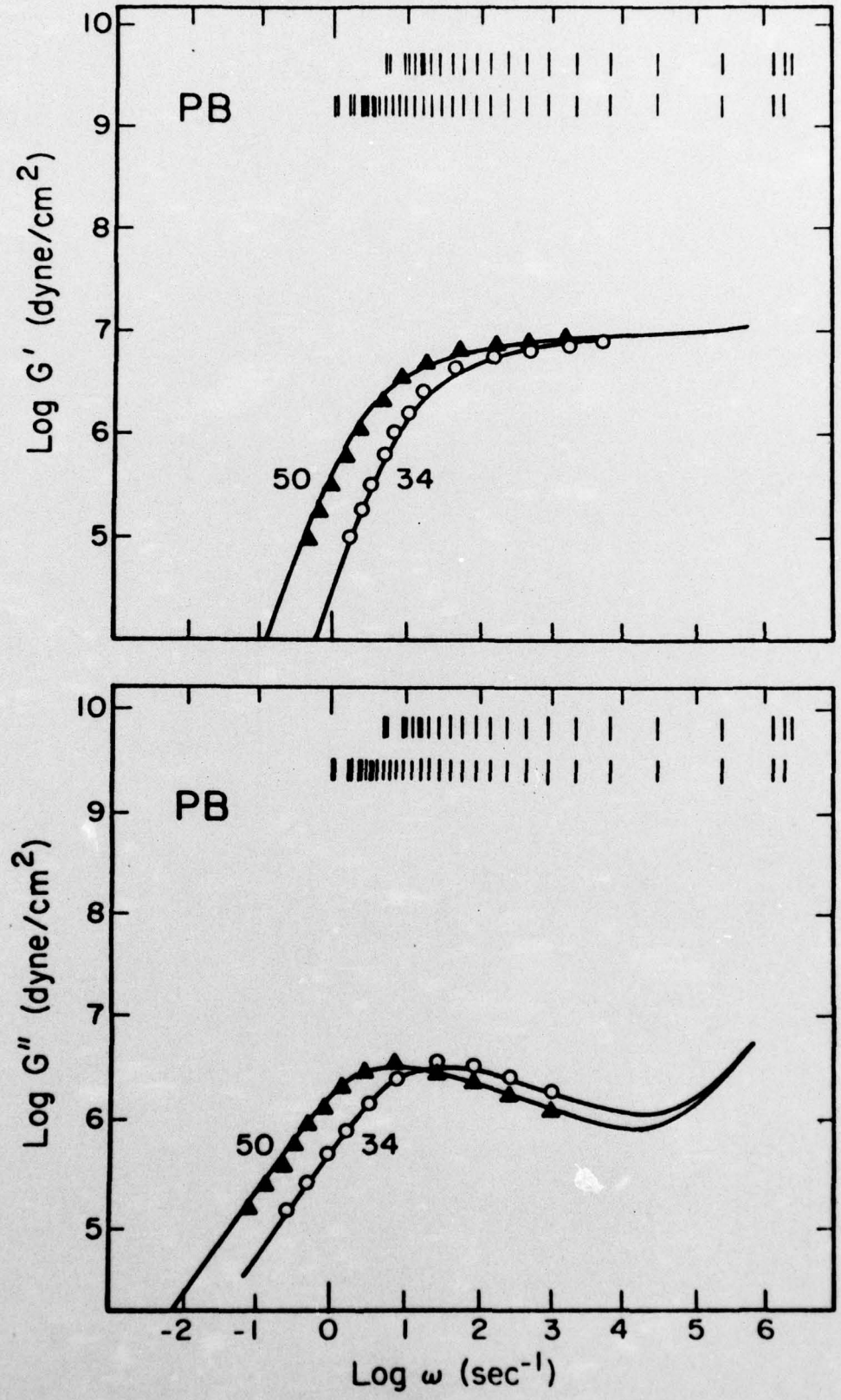

Fig. 11 Dynamic moduli for monodisperse polybutadine (25) for the high-friction-inside case with $\delta_j^{I'} = I^4$ and $\alpha = 0.2$.